Engineering Sciences International Research Journal
ISSN (Print) : 2330 – 4338 ; Volume 1 Issue 1 ǁ February. 2013 ǁ

Hybrid PWM Algorithm for Direct Torque Controlled Induction Motor Drive with Reduced Computationalburden

J. Bhavani[1], J. Amarnath[2], D. Subbarayudu[3]

Abstract: This paper presents a simple and efficient hybrid pulsewidth modulation (HPWM) algorithm for direct torque controlled induction motor drives. In this paper first, a generalized pulse width modulation (GPWM) algorithm is presented, in which, by varying a constant (k_2) value from zero to one, various DPWM algorithms can be generated along with the SVPWM algorithm. As the proposed approach uses instantaneous phase voltages only for the calculation of gating times of the inverter, the complexity burden involved is very less when compared with the classical space vector approach. Then, the rms stator flux ripple, which is a measure of ripple in line current characteristics have been plotted for all the DPWM and SVPWM algorithms. From which, it is concluded that the SVPWM algorithm gives superior performance at lower modulation indices, whereas the DPWM algorithms give superior performance at higher modulation indices. Hence, to achieve the superior waveform quality at all modulation indices, a hybrid PWM (HPWM) algorithm has been presented in this paper. To validate the proposed algorithms, several numerical simulation studies have been carried out and results have been presented and compared.

Keywords: *DPWM, DTC, flux ripple, GPWM, HPWM, PWM, SVPWM.*

1. INTRODUCTION

Nowadays, many researchers have been focused their interest on variable speed drives (VSDs) due to their increasing number of applications. In the high performance drive applications, field oriented control (FOC) and direct torque control (DTC) algorithms are becoming popular. The FOC algorithm gives the decoupling control of torque and flux of an induction motor drive and control the induction motor similar to a separately excited dc motor [1]. But, the complexity involved in the FOC algorithm is more due to reference frame transformations. To reduce the complexity involved, a new control strategy called as direct torque control (DTC) has been proposed in [2]. A detailed comparison between FOC and DTC is presented in [3] and concluded that DTC gives fast torque response when compared with the FOC. Though, FOC and DTC give fast transient and decoupled control, these operate the inverter at variable switching frequency due to hysteresis controllers. Moreover, the steady state ripples in torque, flux and currents are high in DTC.

To reduce the harmonic distortion and to obtain the constant switching frequency operation of the inverter, nowadays many researchers have focused their interest on pulsewidth modulation (PWM) algorithms. A large variety of PWM algorithms have been discussed in [4]. But, the most popular PWM algorithms as sinusoidal PWM (SPWM) and space vector PWM (SVPWM) algorithms. The SVPWM algorithm offers more degrees of freedom when compared with the SPWM algorithms. Hence, it is attracting many researchers. The SVPWM algorithm is explained in detailed in [5]. Though the SVPWM and SPWM algorithms give good performance, these give more switching losses of the inverter due to the continuous modulating signals. Hence, to reduce the switching losses of the inverter, the discontinuous PWM (DPWM) algorithms are becoming popular. Also, the classical SVPWM algorithm requires angle and sector information to generate the actual gating times of the inverter. Hence, the complexity involved is more. To reduce the complexity involved in the algorithms and for easier implementation, nowadays, the carrier based PWM algorithms are attracting many researchers. The magnitude tests based approach is presented to generate the carrier based SVPWM and various DPWM algorithms with reduced complexity in [6]. Also, by distributing the zero state time unequally, various PWM algorithms have been generated in [7]. By adding a generalized zero sequence signal to the voltages various carrier based PWM algorithms have been generated in [8].

To reduce the complexity in the classical SVPWM algorithms and to extend the operation up to over modulation region, various PWM algorithms have been generated in [9]-[11] by using the concept of offset time and duty cycle. By adding the suitable offset time to the imaginary switching times, which are proportional to the instantaneous phase voltages, various PWM algorithms have been generated under both linear and overmodulation regions. Though, the SVPWM and DPWM algorithms give good performance, the SVPWM algorithm gives more harmonic distortion at higher modulation indices when compared with the DPWM algorithms and DPWM algorithm gives more harmonic distortion at lower modulation indices. Hence, to reduce the harmonic distortion at all

modulation indices, a hybrid PWM algorithm approach has been proposed in [12]-[14].

This paper presents a simplified approach for the generation of SVPWM and DPWM algorithms. Then, the rms stator flux ripple characteristics of all PWM algorithms is presented with reduced complexity. Based on the flux ripple characteristics, simplified hybrid PWM (HPWM) algorithm has been presented with reduced harmonic distortion at all modulation indices.

2. 2.SWITHCING SEQUENCES

The proposed GPWM algorithm may be pursued by the definition of a duty cycle or modulating signal for phase *n* (with *n* = a, b and c), which is given as the ratio between pulsewidth and modulation period.

$$V_n^* = \frac{Pulsewidth}{Modualtion \quad period} \tag{1}$$

Once the modulating signal V_n^* is calculated, the ON and OFF times of the inverter-leg devices can be via digital counters and comparators. For example, the duty cycle or modulating signal of SPWM algorithm can be obtained as follows [6]-[7]:

$$V_n^* = \frac{1}{2} + \frac{V_n}{V_{dc}} \ , \ n = a, \text{b and c} \tag{2}$$

where V_n is the instantaneous reference voltage of phase *n* and V_{dc} is the dc-link voltage. In the similar way, the modulating signals of the various DPWM algorithms and SVPWM algorithms can be obtained by adding a suitable zero sequence voltage (V_z) to the instantaneous phase voltages (V_n).

$$V_n^* = k_1 + \frac{V_n + V_z}{V_{dc}} \tag{3}$$

where

$$V_z = k_2[\min(V_n) - \max(V_n)] - \min(V_n) \tag{4}$$

where k_2 is the parameter that takes into account the unequal null-state sharing, can be defined as follows:

$$k_2 = 0.5(1 + \text{sgn}(\cos(3\omega t + \delta)) \tag{5}$$

where sgn(X) is 1, 0 and –1 when X is positive, zero, and negative, respectively. As previously discussed, and k_1 is an additional parameter whose value may be equal to the value of k_2 or be fixed at 0.5. Thus, the proposed approach eliminates the calculation of both the hexagon sector, in which the reference-voltage space vector is located, and the related phase.

In all the other carrier-based techniques, it must be taken $k_1 = k_2$. The standard SVPWM algorithm can be obtained by fixing the k_2 value at 0.5. Similarly, by fixing the k_2 value at 0 and 1, the DPWMMIN and DPWMMAX algorithms can be obtained. By varying the modulation angle δ in (5), various DPWM algorithms can be generated. The DPWM0, DPWM1, DPWM2 and DPWM3 can be obtained for δ = π/6, 0, - π/6 and - π/3 respectively.

The modulating waveforms of sinusoidal PWM (SPWM), SVPWM and all possible DPWM algorithms are given in Fig.1. In the DPWM methods, any one of the phases is clamped to the positive or negative DC bus for utmost a total of 120^0 over a fundamental cycle. Hence, the switching losses of the associated inverter leg are eliminated. Moreover, within a sampling time period three switchings will occur in SVPWM algorithm whereas two switchings in all the above DPWM algorithms. Hence, to maintain constant average switching frequency of the inverter, the frequency of DPWM algorithms is taken as 1.5 times of the switching frequency of the SVPWM algorithm.

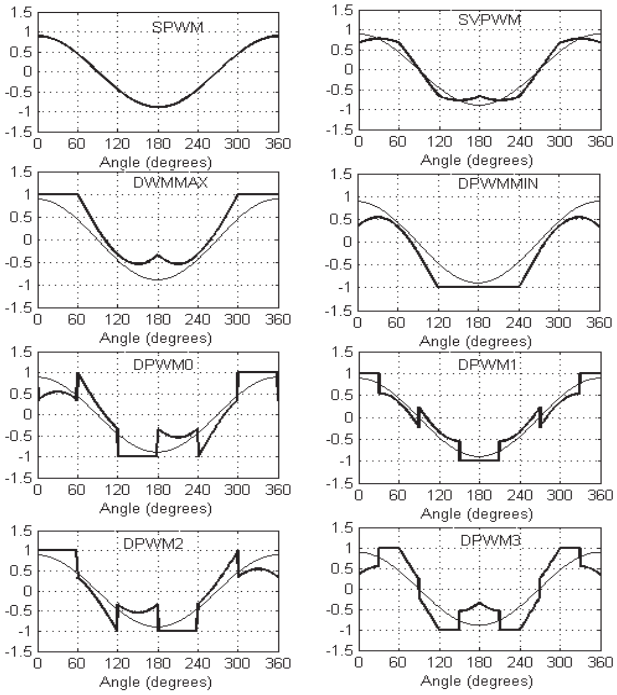

Fig. 1 Modulating waveforms of various PWM methods at M_i = 0.7

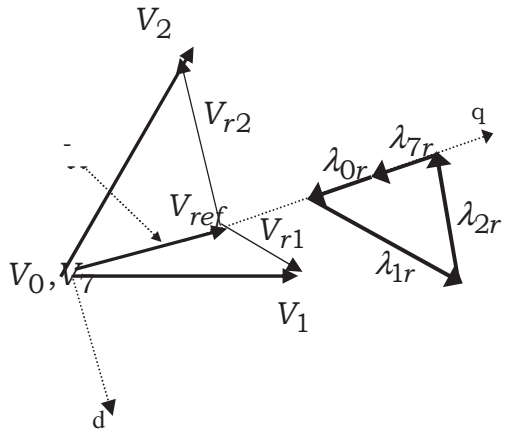

Fig. 2 Voltage ripple vectors and trajectory of the flux ripple.

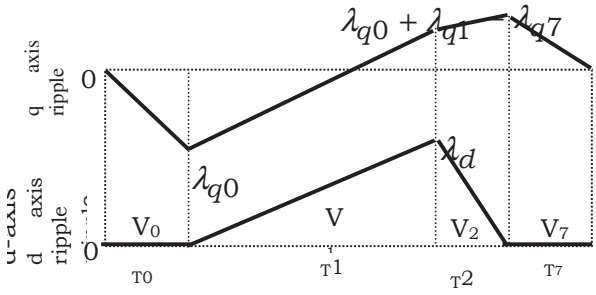

Fig. 3 q-axis and d-axis components of the flux ripple vectors.

3. PROPOSED HYBRID PWM ALGORITHM

The SVPWM algorithm uses equal distribution of zero state times among two zero states. Whereas the proposed GPWM algorithm uses unequal distribution of zero state time and it distributes the zero state time as $T_0 = k_2 T_z, T_7 = (1-k_2)T_z$, where T_z is the total zero state time. In the space vector approach, the applied voltage vector equals the reference voltage vector only in an average sense over the given sampling interval, and not in an instantaneous fashion.

The difference between applied voltage vector and reference voltage vector is the ripple voltage vector, which depends on space and modulation index. The ripple voltage vectors and trajectory of the stator flux ripple can be represented in a complex plane as shown in Fig. 2. The corresponding d-axis and q-axis components of the stator flux ripple vector are as shown in Fig. 3, from which it is observed that the application of a zero voltage vector results in a variation of the q-axis component of the flux ripple and the application of any active voltage vector results in variation of the both the d-axis and q-axis components. The error volt-seconds corresponding to the voltage ripple vectors are given by

$$V_{r1}T_1 = \left(\frac{2}{3}V_{dc}\sin\alpha\right)T_1 + j\left(\frac{2}{3}V_{dc}\cos\alpha - V_{ref}\right)T \tag{6}$$

$$\begin{aligned} V_{r2}T_2 = &-\left(\frac{2}{3}V_{dc}\sin(60^o-\alpha)\right)T_2 \\ &+ j\left(\frac{2}{3}V_{dc}\cos(60^o-\alpha) - V_{ref}\right)T_2 \end{aligned} \tag{7}$$

$$V_{r0}T_0 = -jV_{ref}T_0 = -j\frac{2M_iV_{dc}}{\pi}T_0 = j\lambda_{q0} \tag{8}$$

$$V_{r7}T_7 = -jV_{ref}T_7 = -j\frac{2M_iV_{dc}}{\pi}T_7 = j\lambda_{q7} \tag{9}$$

From the switching times expressions of the classical SVPWM algorithms, by substituting the values of $\sin\alpha$, $\cos\alpha$ and $\cos(60^o-\alpha)$ in (6) - (9), the following expressions can be obtained.

$$\begin{aligned} V_{r1}T_1 &= \frac{\pi V_{dc}}{3\sqrt{3}M_i}\frac{T_1T_2}{T_s} + j\left(\frac{2V_{dc}\pi(T_1+0.5T_2)}{9M_iT_s} - \frac{2V_{dc}M_i}{\pi}\right)T_1 \\ &= \lambda_d + j\lambda_{q1} \end{aligned} \tag{10}$$

$$\begin{aligned} V_{r2}T_2 = &-\frac{\pi V_{dc}}{3\sqrt{3}M_i}\frac{T_1T_2}{T_s} \\ &+ j\left(\frac{2V_{dc}\pi(0.5T_1+T_2)}{9M_iT_s} - \frac{2V_{dc}M_i}{\pi}\right)T_2 \end{aligned} \tag{11}$$

Then the mean square stator flux ripple over a sampling interval can be calculated as

$$\begin{aligned} \lambda^2_{(\mathrm{rms})} &= \frac{1}{T_s}\int_0^{T_s}\lambda_q^2dt + \frac{1}{T_s}\int_0^{T_s}\lambda_d^2dt \\ &= \frac{1}{3}\left\{\lambda_{q0}^2\frac{T_0}{T_s} + \left[\lambda_{q0}^2 + (\lambda_{q0}+\lambda_{q1})^2 + \lambda_{q0}(\lambda_{q0}+\lambda_{q1})\right]\frac{T_1}{T_s}\right. \\ &\quad \left. + \left[(\lambda_{q0}+\lambda_{q1})^2 - \lambda_{q7}(\lambda_{q0}+\lambda_{q1}) + \lambda_{q7}^2\right]\frac{T_2}{T_s}\right. \end{aligned} \tag{12}$$

By using (12), the mean square flux ripple can be easily computed and graphically represented for all PWM methods. The mean square stator flux ripple characteristics obtained from (12) for various PWM algorithms and for different modulation indices are shown in Fig.4 – Fig.7.

From Fig. 4– Fig. 7, it can be observed that replacing α by $(60^o - \alpha)$ in the rms stator flux ripple expressions of SVPWM does not change its value. However, the rms ripple over a subcycle is not symmetric about the center of the sector for the other PWM sequences. Moreover, it can be observed that the DPWM3 algorithm gives less harmonic distortion when compared with the other DPWM algorithms. In order to minimize the harmonic distortion in the line current, the rms current ripple or rms stator flux ripple over every sampling time period should be reduced. The proposed hybrid PWM (HPWM) algorithm employ the best PWM algorithm among the SVPWM and DPWM3 algorithms to minimize the rms current ripple in every sampling time period.

In the proposed HPWM algorithm, in every sampling time period the rms stator flux ripples of SVPWM and DPWM3 are compared with each other and the PWM algorithm, which has less rms stator flux ripple is applied to minimize the THD. Thus, the proposed HPWM algorithm uses the DPWM3 algorithm in conjunction with SVPWM algorithm.

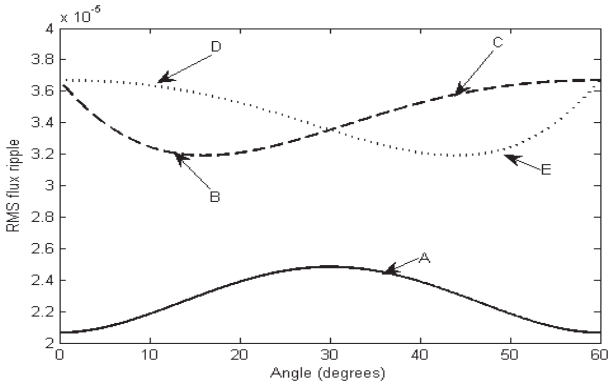

Fig. 4. RMS flux ripple over a subcycle against the angle α at M_i=0.4 (A: SVPWM, CD: DPWM1, BE: DPWM3, DE: DPWMMAX, DPWM2 and BC: DPWMMIN, DPWM0)

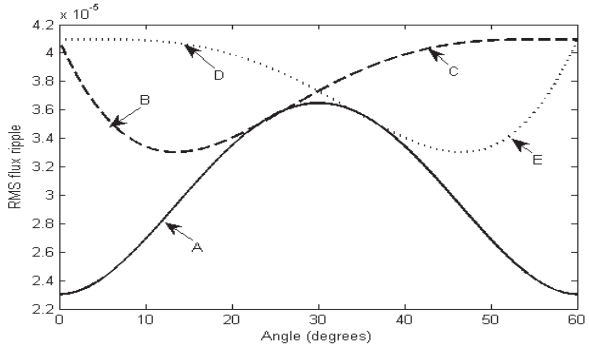

Fig. 5. RMS flux ripple over a subcycle against the angle α at M_i=0.55

(A: SVPWM, CD: DPWM1, BE: DPWM3, DE: DPWMMAX, DPWM2 and BC: DPWMMIN, DPWM0).

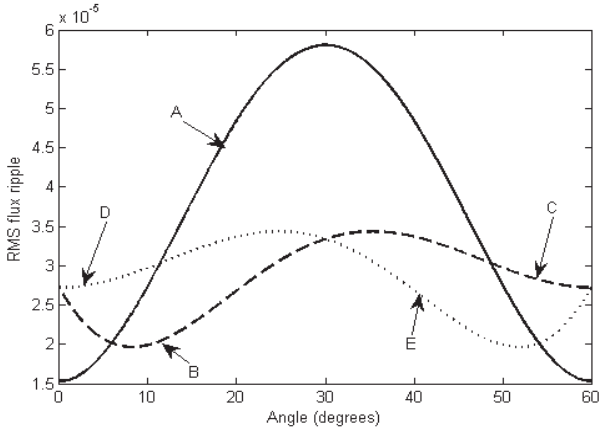

Fig. 6. RMS flux ripple over a subcycle against the angle α at M_i=0.75(A: SVPWM, CD: DPWM1, BE: DPWM3, DE: DPWMMAX, DPWM2 and BC: DPWMMIN, DPWM0)

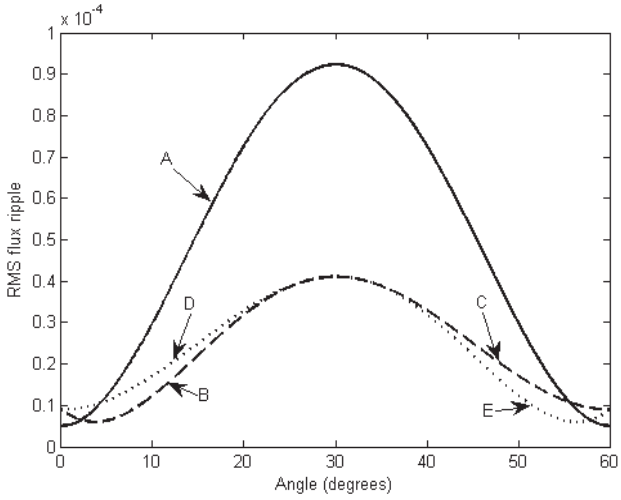

Fig. 7. RMS flux ripple over a subcycle against the angle α at M_i=0.906(A: SVPWM, CD: DPWM1, BE: DPWM3, DE: DPWMMAX, DPWM2 and BC: DPWMMIN, DPWM0).

4. PROPOSED HPWM ALGORITHM BASED DTC

The reference voltage space vector can be constructed in many ways. But, to reduce the complexity of the algorithm, in this thesis, the required reference voltage vector, to control the torque and flux cycle-by-cycle basis is constructed by using the errors between the reference d-axis and q-axis stator fluxes and d-axis and q-axis estimated stator fluxes sampled from the previous cycle. The block diagram of the proposed HPWM based DTC is as shown in Fig.8

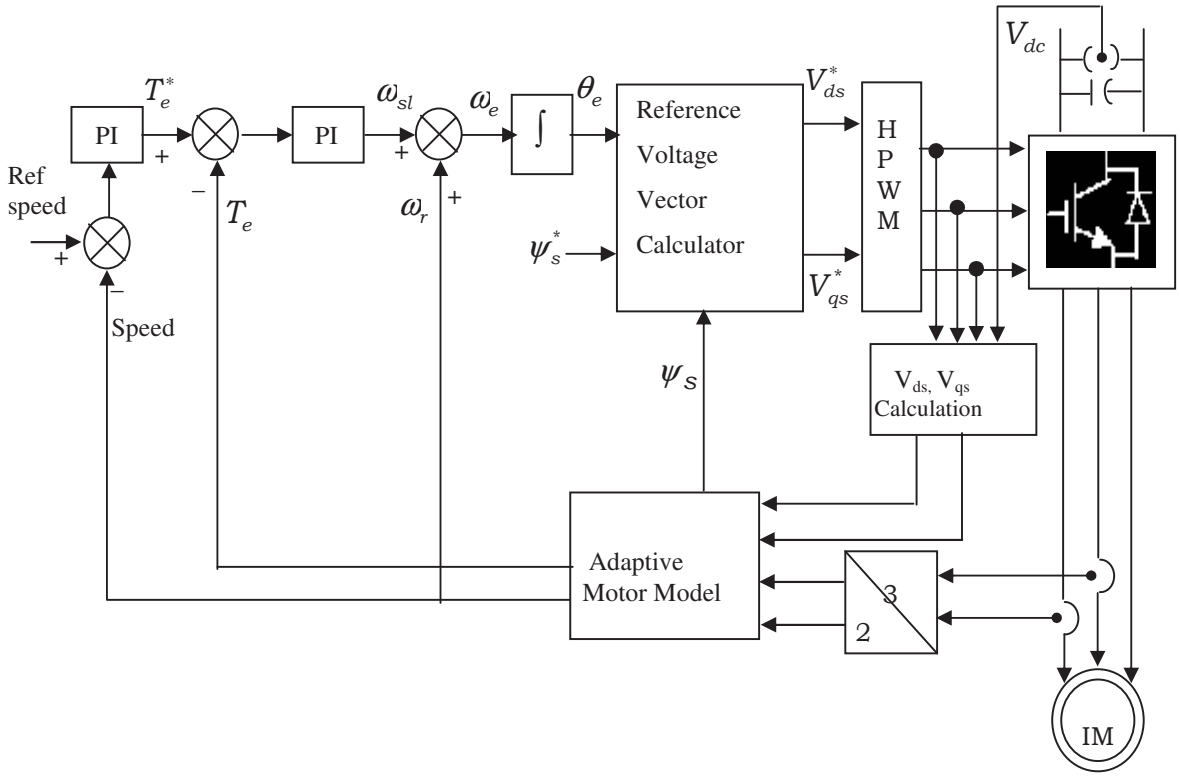

Fig. 8. Block diagram of proposed HPWM based DTC

From Fig.8, it is seen that the proposed HPWM based DTC scheme retains all the advantages of the DTC, such as no co-ordinate transformation, robust to motor parameters, etc. However a space vector modulator is used to generate the pulses for the inverter, therefore the complexity is increased in comparison with the DTC method.

In the proposed method, the position of the reference stator flux vector $\overline{\psi}_s^*$ is derived by the addition of slip speed and actual rotor speed. The actual synchronous speed of the stator flux vector $\overline{\psi}_s$ is calculated from the adaptive motor model.

After each sampling interval, actual stator flux vector $\overline{\psi}_s$ is corrected by the error and it tries to attain the reference flux space vector $\overline{\psi}_s^*$. Thus the flux error is minimized in each sampling interval. The d-axis and q-axis components of the reference voltage vector can be obtained as follows:

Reference values of the d-axis and q- axis stator fluxes and actual values of the d-axis and q-axis stator fluxes are compared in the reference voltage vector calculator block and hence the errors in the d-axis and q-axis stator flux vectors are obtained as in (13)-(14).

$$\Delta\Psi_{ds} = \Psi_{ds}^* - \Psi_{ds} \tag{13}$$

$$\Delta\Psi_{qs} = \Psi_{qs}^* - \Psi_{qs} \tag{14}$$

The appropriate reference voltage space vectors due to flux error and stator ohmic drop are given as

$$v_{ds}^* = R_s i_{ds} + \frac{\Delta\psi_{ds}}{T_s} \tag{15}$$

$$v_{qs}^* = R_s i_{qs} + \frac{\Delta\psi_{qs}}{T_s} \tag{16}$$

Where, T_s is the duration of subcycle or sampling period and it is a half of period of the switching frequency. This implies

that the torque and flux are controlled twice per switching cycle. Further, these d-q components of the reference voltage vector are fed to the SVPWM block from which, the actual switching times for each inverter leg are calculated.

5. SIMULATION RESULTS AND DISCUSSION

To validate the proposed generalized PWM algorithm based DTC, several numerical simulation studies have been carried out and results are presented. The details of the induction motor, which is used for simulation studies are as follows:

A 3-phase, 4 pole, 4kW, 1200rpm induction motor with parameters as follows: R_s = 1.57Ω, R_r = 1.21Ω, L_s = L_r = 0.17H, L_m = 0.165H and J = 0.089Kg.m^2.

The steady state simulation results for SVPWM based DTC are shown from Fig. 9 to Fig. 10. From the harmonic spectra, it can be observed that the SVPWM algorithm gives considerable amplitude of dominating harmonics around switching frequency. Hence, the SVPWM algorithm gives more acoustical noise/electromagnetic interference.

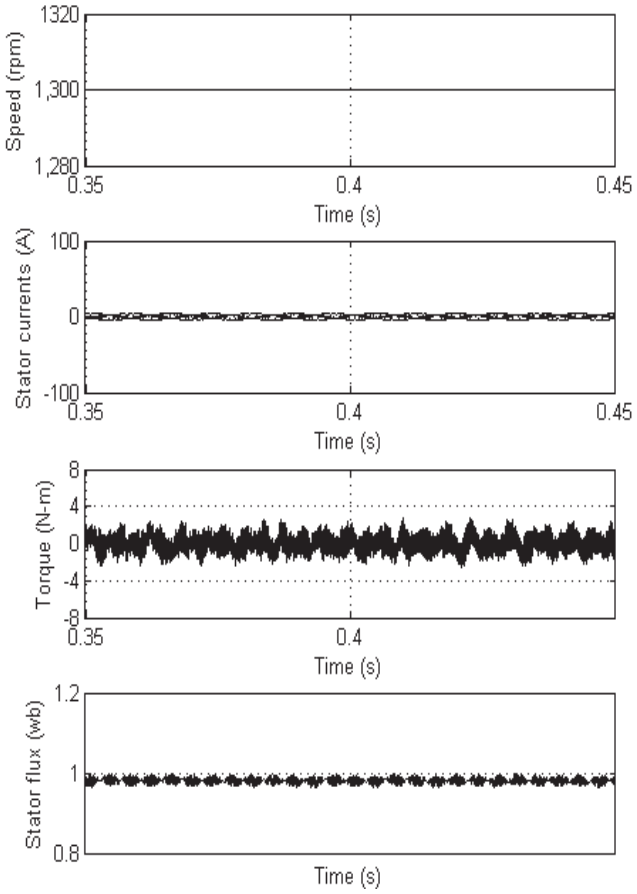

Fig. 9. Steady state simulation results for SVPWM based DTC.

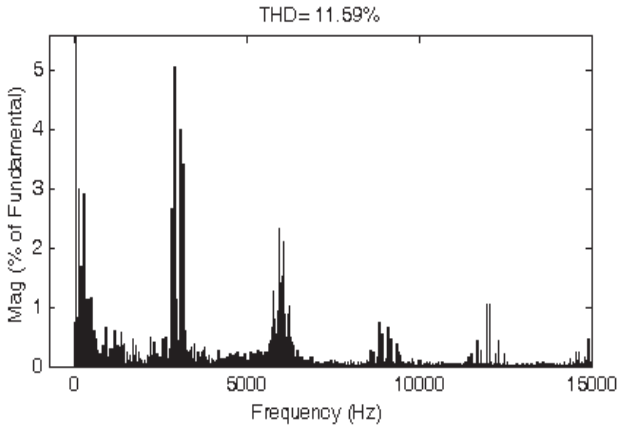

Fig. 10 Harmonic spectra of line current of SVPWM based DTC

The simulation results at various conditions such as starting, steady state, and step-change in load change and speed reversal for proposed HPWM algorithm based DTC are shown from Fig. 11 to Fig. 17. From the simulation results, it can be observed that the proposed PWM algorithm gives good performance when compared with the SVPWM algorithm. Moreover, the proposed HPWM algorithm gives wide spread harmonic spectrum and gives reduced amplitudes of dominating harmonics. Hence, the proposed PWM algorithm gives reduced acoustical noise and reduced harmonic distortion when compared with the SVPWM algorithm.

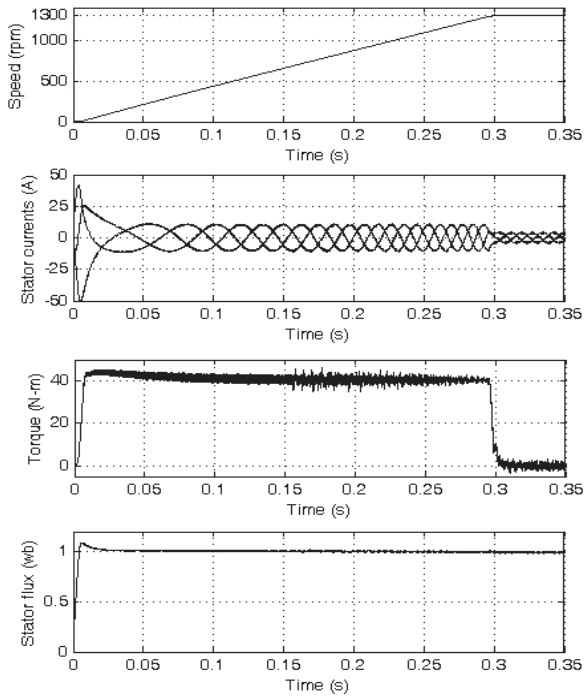

Fig. 11. starting transients in the proposed HPWM based DTC

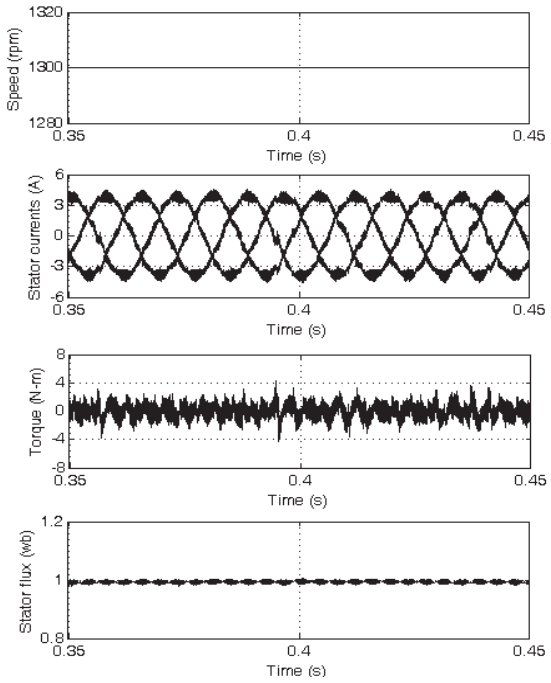

Fig. 12. Steady state simulation results for proposed HPWM Based DTC

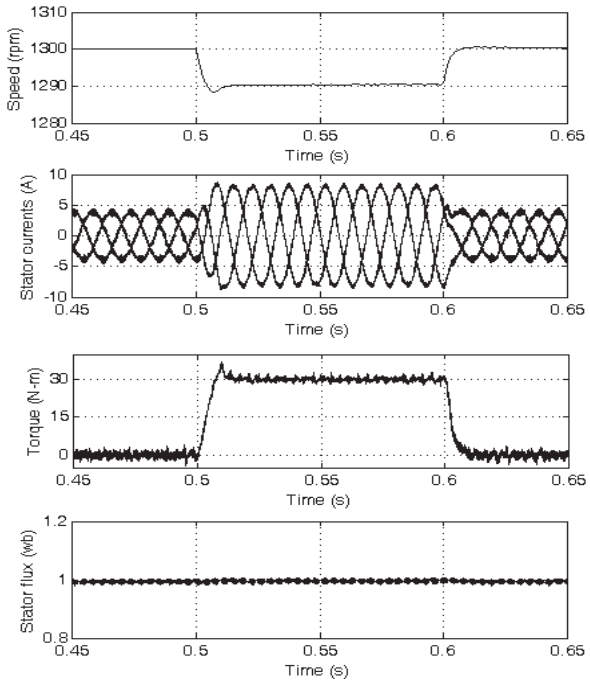

Fig. 15. transients during the step change in load in the proposed HPWM based DTC

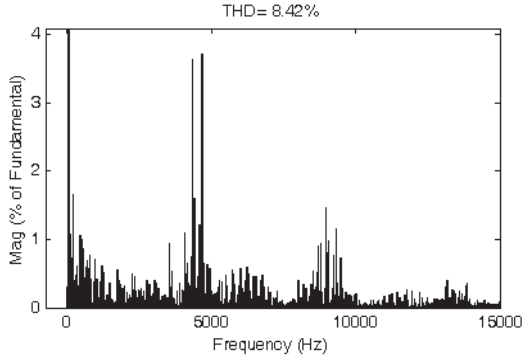

Fig. 13. Harmonic spectra of line current of proposed HPWM based DTC

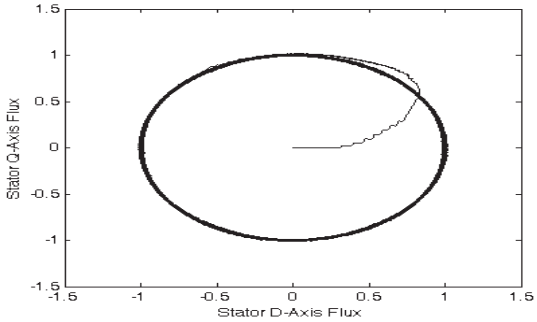

Fig. 14. locus of stator flux in the proposed HPWM based DTC

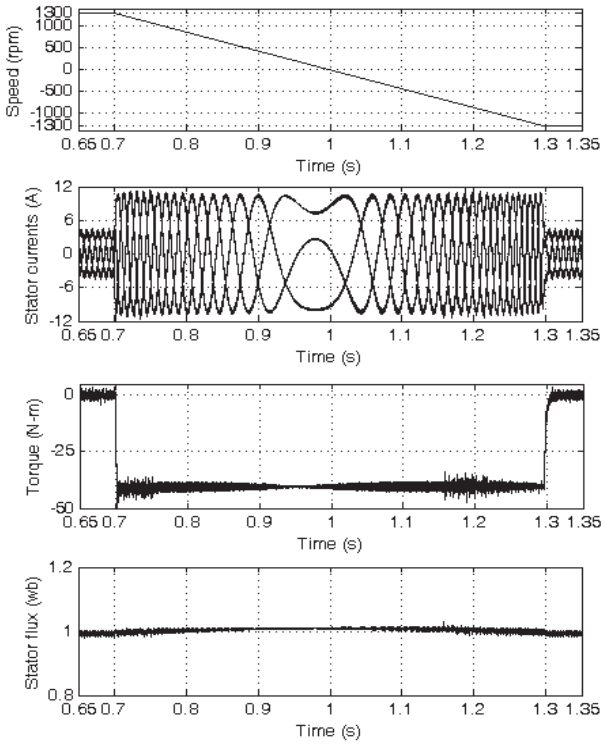

Fig. 16 transients during the speed reversal (speed is changed from +1300 rpm to -1300 rpm) for the proposed HPWM based DTC.

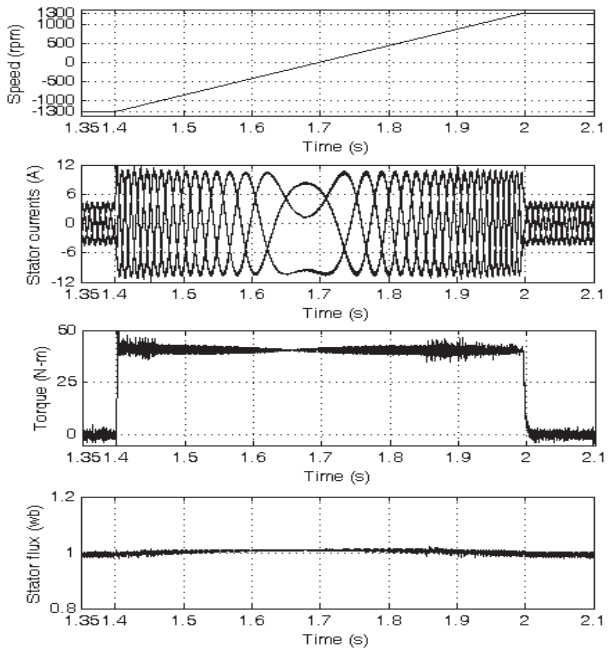

Fig. 17. transients during the speed reversal (speed is changed from -1300 rpm to +1300 rpm) for the proposed HPWM based DTC

6. CONCLUSIONS

A simple and efficient HPWM algorithm has been proposed for DTC based induction motor drives in this paper. As the SVPWM algorithm gives considerable amplitude of dominating harmonics around switching frequency, it generates more acoustical noise and gives more harmonic distortion. Hence, to reduce the acoustical noise and harmonic distortion, a simplified HPWM algorithm is presented in this paper for direct torque controlled induction motor drive. The proposed PWM algorithm selects suitable switching sequence based on the stator flux ripple value. Hence, the proposed PWM algorithm gives spread spectra and gives reduced amplitude of dominating harmonics when compared with the SVPWM algorithm. The simulation results confirm the effectiveness of the proposed PWM algorithm.

7. REFERENCES

[1] Domenico Casadei, Francesco Profumo, Giovanni Serra, and Angelo Tani, "FOC and DTC: Two Viable Schemes for Induction Motors Torque Control" *IEEE Trans. Power Electron.,* vol. 17, no.5, Sep, 2002, pp. 779-787.

[2] Joachim Holtz, "Pulsewidth modulation – A survey" IEEE Trans. Ind. Electron., vol. 39, no. 5, Dec 1992, pp. 410-420.

[3] Heinz Willi Van Der Broeck, Hans-Christoph Skudelny and Georg Viktor Stanke, "Analysis and realization of a Pulsewidth Modulator based on Voltage Space Vectors", IEEE Trans. Ind. Applic., Vol. 24, No.1, Jan/Feb 1988, pp.142-150.

[4] Ahmet M. Hava, Russel J. Krkman and Thomas A. Lipo, "Simple analytical and graphical methods for carrier-based PWM-VSI drives" IEEE Trans. Power Electron., vol. 14, no. 1, Jan 1999, pp. 49-61.

[5] V. Blasko, "Analysis of a hybrid PWM based on modified space-vector and triangle-comparison method," IEEE Trans. Ind. Applicat., vol. 33, pp. 756–764, May/Jun, 1997.

[6] Olorunfemi Ojo, "The generalized discontinuous PWM scheme for three-phase voltage source inverters" IEEE Trans. Ind. Electron., vol. 51, no. 6, Dec, 2004, pp. 1280-1289.

[7] V. Blasko, "Analysis of a hybrid PWM based on modified space-vector and triangle-comparison method," IEEE Trans. Ind. Applicat., vol. 33, pp. 756–764, May/Jun, 1997.

[8] Olorunfemi Ojo, "The generalized discontinuous PWM scheme for three-phase voltage source inverters" IEEE Trans. Ind. Electron., vol. 51, no. 6, Dec, 2004, pp. 1280-1289.

[9] Dae-Woong Chung, Joohn-Sheok Kim, Seung-Ki Sul, "Unified Voltage Modulation Technique for Real-Time Three-Phase Power Conversion" IEEE Trans. On Ind. Applications, vol. 34, no.2, pp 374-380, March/April, 1998, pp. 756-764.

[10] Antonio Cataliotti, Fabio Genduso, Angelo Raciti, and Giuseppe Ricco Galluzzo "Generalized PWM–VSI Control Algorithm Based on a Universal Duty-Cycle Expression: Theoretical Analysis, Simulation Results, and Experimental Validations" *IEEE transactions on Ind. Electron.*, vol. 54, NO. 3, June 2007, pp 1569-1580.

[11] Edison Roberto C. Da Silva, Euzeli CiprianoDos Santos, Jr., and Cursino Bradao Jacobina, "Pulsewidth modulation strategies" *IEEE Ind. Electron., Magazine,* no.2, pp.37-45, June, 2011.

[12] H. Krishnamurthy, G, Narayanan, V.T.Ranganathan, R. Ayyar, "Design of space vector-based hybrid PWM techniques for reduced current ripple" IEEEAPEC, Vol.1, pp 583-588, 2003.

[13] G.Narayanan, Di Zhao, H. Krishnamurthy and Rajapandian Ayyanar, "Space vector based hybrid techniques for reduced current ripple" IEEE Trans. Ind. Applic., Vol. 55, No.4, pp.1614-1626, April 2008.

[14] T. Brahmananda Reddy, J. Amarnath and D. Subbarayudu, "Improvement of DTC performance by using hybrid space vector Pulsewidth modulation algorithm" International Review of Electrical Engineering, Vol.4, no.2, pp. 593-600, Jul-Aug, 2007.

[15] N. Ravisankar Reddy, T. Brahmananda Reddy, J. Amarnath, and D. Subba Rayudu "Hybrid PWM Algorithm for Vector Controlled Induction Motor Drive without Angle Estimation for Reduced Current Ripple" ICGST-ACSE journal, vol 9, issue 3, pp.41-49, Dec 2009.

* * *

[1]*J.Bhavani, Associate professor, EEE Department, KL University,Vaddeswaram,Vijayawada, Andhra Pradesh,India*
[2]*J.Amarnath, Professor, EEE Department, JNTUH College of Engineering ,kukatpally Hyderabad, Andhra Pradesh,India.*
[3]*D. Subba Rayudu, Professor, EEE Department, Pulla Reddy Engineering College, Kurnool, A.P, India*
[1]*bhavanisekhar2004@hotmail.com,* [2]*amarnathjinka@yahoomail.com,* [3]*subbarayudu@rediffmail.com*